energies

MDPI

Article

Similitude Analysis of Experiment and Modelling of Immiscible Displacement Effects with Scaling and Dimensional Approach

Andrzej Gołąbek [1,*], Wiesław Szott [1], Piotr Łętkowski [1] and Jerzy Stopa [2]

[1] Oil and Gas Institute–National Research Institute, Lubicz 25A, 31-503 Krakow, Poland; szott@inig.pl (W.S.); letkowski@inig.pl (P.Ł.)

[2] Department of Petroleum Engineering, AGH University of Science and Technology, al. Mickiewicza 30, 30-059 Krakow, Poland; stopa@agh.edu.pl

* Correspondence: golabek@inig.pl; Tel.: +48-134368941

Received: 11 September 2020; Accepted: 5 October 2020; Published: 7 October 2020

Abstract: This paper presents the use of scaling and dimensional analysis to assess the viability of conventional modelling of immiscible displacement occurring when water is injected into the oil-saturated, porous rock—a conventional secondary oil-recovery method. A brief description of the laboratory tests of oil displacement with water performed on long core sets taken from wells operating on a Polish oil reservoir was presented. A dimensionless product generator based on dimensional analysis and Buckingham Π theorem was used to generate all possible combinatorial sets of dimensionless products for physical variables describing the phenomenon. The mathematical model of the phenomenon was transformed to its dimensionless form, using a selected set of the products. The results of the laboratory tests were analyzed as functions of the products. Statistically verified quantities describing both dependent and independent experiment variables were subject to a regression analysis to study dependencies of the experimental results upon selected dimensionless products. The degrees of the dependencies were determined and compared with the model coefficients. The conclusions are drawn for the purposes of model application to correctly describe the laboratory and, consequently, field scale processes of immiscible oil displacement by water.

Keywords: immiscible displacement; mathematical modelling; scaling; dimensional analysis; dimensionless products; regression analysis; similitude

1. Introduction

Immiscible displacement is a phenomenon occurring, e.g., during the process of water injection to an oil field as a secondary method of oil recovery [1,2]. Effectiveness of this phenomenon is estimated in laboratories by performing experiments on bore-hole cores [3,4]. The obtained results of laboratory tests are typically used to model this phenomenon with full-scale reservoir models [5,6]. However, to quantitatively characterize the phenomenon, it is necessary to apply appropriate models of laboratory experiments. To the authors' best knowledge, there are relatively few papers reporting immiscible displacement experimental results associated with their modelling and analyses of its correctness [7,8]. This paper presents a unique report on the subject with regard to the carbonate rocks and reservoir fluids found in Polish petroleum formations.

Both small- and large-scale modelling are conventionally performed by an approximate description of the real-world phenomena. To assess the viability of such modelling, a scaling and dimensional analysis is performed as applied to the immiscible flow data obtained from the laboratory experiments. Scaling laws are derived by dimensional analysis from the general standpoint according to the Buckingham Π theorem [9].

This theorem says that every function with n dimensional parameters a_i, $i = 1, 2, \ldots, n$, of which k has basic dimensions, can be represented as a function of $n-k$ dimensionless parameters of the following type: $\Pi_j = a_1^{p_{1,j}} a_2^{p_{2,j}} \ldots a_n^{p_{n,j}}$, $j = 1, 2, \ldots, n-k$, where exponents $p_{i,j}$ are rational numbers. The theorem provides a method for conversion of a physically meaningful equation involving n physical variables $f(a_i, a_2, \ldots, a_n) = 0$ into a new equation $F(\Pi_1, \Pi_2, \ldots, \Pi_{n-k}) = 0$ of $n-k$ dimensionless Π_j, $j = 1, 2, \ldots, n-k$. The Buckingham Π theorem states that validity of the laws of physics does not depend on a specific unit system. It should be noticed that choice of dimensionless parameters is not unique. However, the theorem provides a method for computing sets of dimensionless parameters from the given variables even if the form of the equation $f(a_i, a_2, \ldots, a_n) = 0$ is unknown.

If the Π parameters are identical for two different systems, then the phenomenon will proceed in the same way, despite different a_i parameters. The parameters of the Π type is therefore called similarity parameters or criteria of similarity.

Thus, Buckingham Π theorem allows for the reduction of the most general equations of physical variables that describe the phenomenon to equations involving only sets of dimensionless products (Π's) constructed from the original variables. The significance of the dimensionless Π products is then analyzed with respect to their influence upon experimental results and confronted with the dependencies of the model. If it is positively verified, the model can be applied to the large-scale problems, according to the similarity theory [10]. This theory is used mainly in the fluid mechanics [11], hydraulics [12], and aerodynamics [13]. In the area of the fluid mechanics, there are several specific Π products known for their unique names, such as the Reynolds number, *Re* [14], and Weber number, *We* [15]. They have well-defined physical interpretation. The former is the ratio of inertial forces to viscous forces, and the latter is a measure of fluids inertia compared to their interfacial tension.

In this paper, we apply the procedure introduced above, to assess the viability of conventional modelling of immiscible fluid displacement as used in oil reservoir simulations and implemented in all commercial simulators. The procedure is applied to the analysis of a set of laboratory tests performed on bore-hole cores. A detailed description of the procedure is presented, and the appropriate conclusions are drawn.

2. Laboratory Tests

This paper takes advantage of the results of five laboratory tests of oil displacement by water performed on various long core sets [16]. Each set consisted of four cores arranged according to diminishing permeability. The cores were of constant sizes: 2.5 cm in diameter and 5 cm in length. The cores in the first four tests featured similar permeability parameters, ranging between 30 and 60 mD, while in test No. 5, cores with a bigger permeability (up to 400 mD) were used. Prior to starting the displacement tests, all cores were saturated with water and then with oil, to take the irreducible water into account in tests and to estimate the effective porosity of the cores.

Displacement experiments differed between themselves in the rate and total volume of injected water. In tests No. 1 and No. 2, water was injected at the rate of 0.05 cm^3/min, and altogether 1.06 of the cores pore volume (PV) was injected. In tests No. 3 and No. 4, water was injected at the same rate as in previous tests, while altogether 1.09–1.10 of the cores PV was injected. Test No. 5 differed from the others in the injection rate, which was 0.03 cm^3/min, and, in a total 1.08 of the cores, PV was injected into it. The same reservoir fluids of known properties were used in all the tests. The tests were performed under constant initial and outflow pressure (a boundary condition) of $P_{ini} = P_{out} = 424$ bars and constant temperature of $T = 119$ °C. The other boundary condition referred to the constant injection rate at the inflow end of the core sets.

A list of physical variables describing displacement experiments in relation to the laboratory tests, together with the variable dimensions, is shown in Table 1.

Table 1. List of physical variables, together with their dimensions.

Variable		Unit	Dimension Type
position	x	cm	L
time	t	s	t
water permeability at residual oil saturation	k_{wro}	mD	L^2
oil permeability at irreducible water saturation	k_{orw}	mD	L^2
oil pressure	P_o	bar	M/Lt^2
water pressure	P_w	bar	M/Lt^2
water viscosity	μ_w	cP	M/Lt
oil viscosity	μ_o	cP	M/Lt
oil density	ρ_o	g/cm^3	M/L^3
water density	ρ_w	g/cm^3	M/L^3
injection velocity	$v_{w,inj}$	cm/s	L/t
interface tension	σ	dyne/cm	M/t^2
absolute permeability	k	mD	L^2

As the pressure variation in the core sets was relatively low (below 1.2 bar, equivalent to approx. 0.003 of the initial pressure, P_{ini}) during the experiments, the above variables of viscosity, μ, density, ρ, and interfacial tension, σ, determined in Reference [17], were treated as constant values. The relative permeabilities for reservoir oil and water were determined from separate measurements on rock samples of the same formation [17]. It should be noted that the rock of the cores is water-wet [17]. As the injected water used in the tests is the original reservoir water, no changes of core wettability are expected.

Because the considered experiments are carried out on batteries of cores with a diameter much lower than their lengths and the boundary conditions (the injection rate at the inflow end and the pressure at the outflow end) were assumed to be transversely constant, the fluid flow can be modelled as a 1D phenomenon in first approximation. Consequently, only one parameter related to the position dimension was among parameters affecting this displacement phenomenon, i.e., the length of the core batteries—L.

The next parameters include the following: the final time of experiment performance—t; averaged properties of cores—their porosities, ϕ (not specified in Table 1, as they are dimensionless); absolute permeabilities—k; and phase permeabilities of oil and water defined at the residual saturations of reservoir fluids.

Other parameters, describing the process of oil displacement with water, apply to properties of reservoir fluids, such as the phase pressures, viscosities, densities, and interface tension. The last considered parameter, substantially affecting the performed experiments, was the water injection velocity—$v_{w,inj}$, calculated directly from the injection rate divided by the area of the core cross-section.

The main results of the analyzed laboratory tests consisted in the obtained oil outflow and the displacement coefficient as functions of the injection time. The characteristic displacement coefficient at 1 PV of injected water amounted to 56.1%, 56.7%, 56.9%, 56.5%, and 52.8% in test Nos. 1, 2, 3, 4, and 5, respectively.

3. Dimensionless Π Products for Immiscible Displacement

A universal generator of Π products was developed based on the Buckingham Π theorem. The algorithm implemented in the generator was adopted from the literature [18]. Figure 1 presents the block diagram of this algorithm. Moreover, Π products are generated from all possible combinations (without repetition) of dimensional variables, a_i, of different dimensions by writing out k-element string from the n-element a_i set. Every k-element string is a base of the whole Π product set. Every such set is generated by complementing k-element string with one of the $n-k$ remaining elements of the a_i set. Thus, there are $n-k$ quantities equal to the products of $k+1$ dimensional variables a_i, each raised to an exponent that is determined from the condition of Π being dimensionless with respect to each of

the k basic dimensions. This algorithm results in $\begin{pmatrix} n \\ k \end{pmatrix}$ sets containing $n - k$ dimensionless Π products; however, the effective number of the sets is smaller than $\begin{pmatrix} n \\ k \end{pmatrix}$, as some of the original sets are identical.

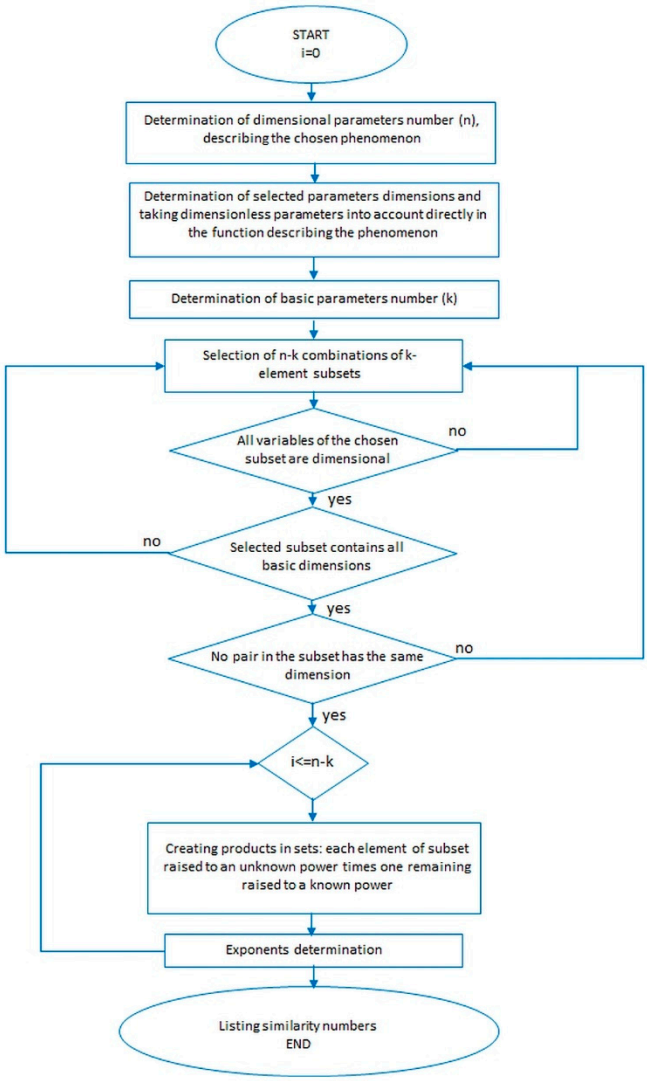

Figure 1. Block diagram of the algorithm for criterial numbers generation.

In the analyzed case of immiscible displacement, input variables of the algorithm included the list of $n = 13$ physical variables from Table 1, and basic $k = 3$ dimensions from which the dimensions of these variables are derived, i.e., L—length, M—mass, and t—time. Therefore, according to the Buckingham theorem, ten $(n - k)$ Π_i parameters, where $i = 1, 2, \ldots, 10$ can be defined to describe the immiscible displacement experiments.

Altogether there are 173 possible sets of Π products for immiscible displacement that were generated. Table 2 presents examples of six sets which were used in the further analysis where the basic model equations applied to describe the phenomenon were transformed to a dimensionless form.

Table 2. Generated sets of products Π (selected for analysis).

Set No. 17		**Set No. 78**		**Set No. 131**	
Π_1	$L/(k_{wro}{}^{0.5})$	Π_1	vt/L	Π_1	$(\rho_w{}^{0.5})L/(t^{0.5})(\mu_o{}^{0.5})$
Π_2	$tv_{w,inj}/L$	Π_2	k_{wro}/L^2	Π_2	$\rho_w k_{wro}/(t\mu_o)$
Π_3	k_{orw}/k_{wro}	Π_3	k_{orw}/L^2	Π_3	$\rho_w k_{ocw}/(t\mu_o)$
Π_4	$(k_{wro}{}^{0.5})P_o/\sigma$	Π_4	$LP_o/(\mu_o v_{w,inj})$	Π_4	tP_o/μ_o
Π_5	$(k_{wro}{}^{0.5})P_w/\sigma$	Π_5	$LP_w/(\mu_o v_{w,inj})$	Π_5	tP_w/μ_o
Π_6	$\sigma k/[\mu_w v_{w,inj} L(k_{wro})^{0.5}]$	Π_6	μ_w/μ_o	Π_6	μ_w/μ_o
Π_7	$\sigma k/[\mu_o v_{w,inj} L(k_{wro})^{0.5}]$	Π_7	$v_{w,inj}L\rho_o/\mu_o$	Π_7	ρ_o/ρ_w
Π_8	$(v_{w,inj}{}^2)(k_{wro}{}^{0.5})\rho_o/\sigma$	Π_8	$v_{w,inj}L\rho_w/\mu_o$	Π_8	$(t^{0.5})(\rho_w{}^{0.5})v_{w,inj}/(\mu_o{}^{0.5})$
Π_9	$(v_{w,inj}{}^2)(k_{wro}{}^{0.5})\rho_w/\sigma$	Π_9	$\sigma/\mu_o v_{w,inj}$	Π_9	$(t^{0.5})(\rho_w{}^{0.5})\sigma/(\mu_o{}^{1.5})$
Π_{10}	$k_{wro}\ \phi/k$	Π_{10}	k/L^2	Π_{10}	$\rho_w k/(t\mu_o)$
Set no. 173		**Set no. 151**		**Set no. 65**	
Π_1	$L/(k_{wro}{}^{0.5})$	Π_1	$L/(k^{0.5})$	Π_1	$L/(k^{0.5})$
Π_2	$v_{w,inj}t/(k_{wro}{}^{0.5})$	Π_2	$v_{w,inj}t/(k^{0.5})$	Π_2	$v_{w,inj}t/(k^{0.5})$
Π_3	k_{orw}/k_{wro}	Π_3	k_{wro}/k	Π_3	k_{wro}/k
Π_4	$(k_{wro}{}^{0.5})P_o/(v\mu_w)$	Π_4	k_{orw}/k	Π_4	k_{orw}/k
Π_5	$(k_{wro}{}^{0.5})P_w/(v\mu_w)$	Π_5	$(k^{0.5})P_o/\sigma$	Π_5	$P_o/(\rho_o v_{w,inj}{}^2)$
Π_6	μ_o/μ_w	Π_6	$(k^{0.5})P_w/\sigma$	Π_6	$P_w/(\rho_o v_{w,inj}{}^2)$
Π_7	$(k_{wro}{}^{0.5})v_{w,inj}\rho_o/\mu_w$	Π_7	$v_{w,inj}\mu_w/\sigma$	Π_7	$\mu_w/(\rho_o v_{w,inj}k^{0.5})$
Π_8	$(k_{wro}{}^{0.5})v_{w,inj}\rho_w/\mu_w$	Π_8	$v_{w,inj}\mu_o/\sigma$	Π_8	$\mu_o/(\rho_o v_{w,inj}k^{0.5})$
Π_9	$\sigma/(v_{w,inj}\mu_w)$	Π_9	$(v_{w,inj}{}^2)(k^{0.5})\rho_o/\sigma$	Π_9	ρ_w/ρ_o
Π_{10}	k/k_{wro}	Π_{10}	$(v_{w,inj}{}^2)(k^{0.5})\rho_w/\sigma$	Π_{10}	$\sigma/(\rho_o v_{w,inj}{}^2k^{0.5})$

4. Immiscible Displacement Equations

Representation of a mathematical model in a dimensionless form enables determination of coefficients, on which this model depends. Equations, conventionally referred to in the case of immiscible displacement in the water–oil system, are the two following differential equations resulting from the equation of continuity and from the Darcy's law [19]:

$$\phi\frac{\partial S_w}{\partial t} = \frac{1}{\mu_w}\vec{\nabla}\cdot\left(k_w\vec{\nabla}\Phi_w\right) \tag{1}$$

$$\phi\frac{\partial S_o}{\partial t} = \frac{1}{\mu_o}\vec{\nabla}\cdot\left(k_o\vec{\nabla}\Phi_o\right) \tag{2}$$

supplemented with the saturation confining relationship:

$$S_o + S_w = 1 \tag{3}$$

oil/water potential definitions:

$$\Phi_{o/w} = P_{o/w} - \rho_{o/w}gz \tag{4}$$

and capillary pressure definition:

$$P_c = P_o - P_w \tag{5}$$

where ϕ—porosity; $S_{w,o}$—water/oil saturation; t—time; $\mu_{w/o}$—water/oil viscosity; x, y, z—coordinates; $k_{w/o}$—water/oil phase permeability; $\Phi_{w/o}$—water/oil potential; $P_{o/w}$—water/oil phase pressure; P_c—capillary pressure; $\rho_{o/w}$—water/oil density; $\Delta\rho$—difference of fluids density; and g—acceleration of gravity.

In the 1D horizontal case, the gravity term in the formulae for potentials is neglected, and the above equations take the following form:

$$\phi\frac{\partial S_w}{\partial t} = \frac{k}{\mu_w}\frac{\partial}{\partial x}\left(k_{rw}\frac{\partial P_w}{\partial x}\right) \tag{6}$$

$$\phi \frac{\partial S_o}{\partial t} = \frac{k}{\mu_o} \frac{\partial}{\partial x} \left(k_{ro} \frac{\partial P_o}{\partial x} \right) \tag{7}$$

$$S_o + S_w = 1 \tag{8}$$

$$P_o = P_w + P_c \tag{9}$$

Here, the porosity, ϕ, and permeability, k, are assumed constant and equal to their average values. Moreover, the pressure dependence of viscosities, $\mu_{o/w}$, is assumed negligibly small, and corresponding terms in (6) and (7) are omitted.

Transformation of the discussed mathematical model to a dimensionless form was performed by using various sets of dimensionless variables' definitions. The most convenient and natural one turned out to be the following:

- time: $t^* = t \frac{v_{w,inj}}{L\, \phi (1 - S_{wr})}$; where $v_{w,inj}$—injection velocity, L—cores length, and S_{wr}—residual water saturation;
- position: $x^* = x \frac{1}{L}$;
- fluids saturations: $S_w^* = \frac{S_w - S_{wr}}{1 - S_{wr}}$, $S_o^* = 1 - S_w^*$;
- oil/water pressure:

$$P_{o/w}^* = P_{o/w} \frac{(k_{wro})^{0.5}}{\sigma};$$

- capillary pressure (J-Leverette function): $J(S_w^*) = \frac{P_c}{\sigma} \left(\frac{k}{\phi} \right)^{0.5}$.

While the definitions of dimensionless position, time, and saturations were of natural and conventional type, those of the pressures were more arbitrary and related to the sets of Π products of Table 2.

Using the above definitions, the Equations (6)–(9) are transformed to the dimensionless form of (10)–(13):

$$\frac{\partial S_w^*}{\partial t^*} = \left(\frac{\sigma k}{\mu_w v_{w,inj} L (k_{wro})^{0.5}} \right) \frac{\partial}{\partial x^*} \left(k_{rw} \frac{\partial P_w^*}{\partial x^*} \right) \tag{10}$$

$$\frac{\partial S_o^*}{\partial t^*} = \left(\frac{\sigma k}{\mu_o v_{w,inj} L (k_{wro})^{0.5}} \right) \frac{\partial}{\partial x^*} \left(k_{ro} \frac{\partial P_o^*}{\partial x^*} \right) \tag{11}$$

$$S_o^* + S_w^* = 1 \tag{12}$$

$$P_o^* = P_w^* + J(S_w^*) \left(\frac{k_{wro} \phi}{k} \right)^{0.5} \tag{13}$$

Here, the interface tension, σ, is assumed to be a negligible function of the water saturations, S_w, in the observed range of $S_{wr} < S_w < 1 - S_{or}$.

As a result of the above transformation, three dimensionless coefficients of Equations (10), (11), and (13), i.e., $\left(\frac{\sigma k}{\mu_w v_{w,inj} L (k_{wro})^{0.5}} \right)$, $\left(\frac{\sigma k}{\mu_o v_{w,inj} L (k_{wro})^{0.5}} \right)$, and $\left(\frac{k_{wro} \phi}{k} \right)^{0.5}$, are identified as Π products of Set No. 17, i.e., Π_6,Π_7, and Π_{10}.

We assume that two systems (the real one and mathematical model) are similar, and the model is scalable when the following are present:

- Dimensionless initial and boundary conditions in the model and in the real system are identical;
- Relative permeabilities k_{rw}, k_{ro} and the function $J(S_w^*)$ are the same functions in the model and in the real system, where $k_{rw} = \frac{k_w}{k}$, $k_{ro} = \frac{k_o}{k}$;
- The assumed dimensionless parameters are the same function of the reduced water saturation, S_w^*, in both systems, from which it results that P_o^*, P_w^*, S_o^*, and S_w^* are the same functions of t^* and x^*.

5. Model Parameters

Characteristic parameters that describe the model used to simulate laboratory tests are listed as M_i, i = 1 to 7, on the right part of Table 3. M_1 and M_2 are independent variables that characterize spatial and temporal results of the tests. As no measurements were done for intermediate positions ($0 < x^* < 1$), M_1 is not used for further analysis. M_2 describes test results as a function of time and is used to analyze time-dependent measurements, such as total reservoir fluid outflow. Parameters M_3 and M_4 refer to initial conditions of the experiments that were fixed for all the experiments. Parameters M_5, M_6, and M_7 are essential coefficients of the model Equations (9), (10), and (12), respectively.

Table 3. Dimensionless parameters of the 1D immiscible displacement process. On the left is the generated set of products, and on the right are the parameters on which model results depend.

Set No. 17		Variability in Experiments	Model Parameters		Comment
Π_1	$L/(k_{wro}{}^{0.5})$	−	M_1	$x^* = x/L$	Independent var., boundary conditions
Π_2	$tv_{w,inj}/L$	+	M_2	$t^* = tv_{w,inj}/L$	Independent var., initial, final conditions
Π_3	k_{ocw}/k_{wro}	−	M_3	$(k_{wro}{}^{0.5})P_{o,ini}/\sigma$	Initial conditions
Π_4	$(k_{wro}{}^{0.5})P_{o,ini}/\sigma$	−	M_4	$(k_{wro}{}^{0.5})P_{w,ini}/\sigma$	Initial conditions
Π_5	$(k_{wro}{}^{0.5})P_{w,ini}/\sigma$	−	M_5	$\sigma k/[\mu_w v_{w,inj} L(k_{wro})^{0.5}]$	Equation coefficient
Π_6	$\sigma k/[\mu_w v_{w,inj} L(k_{wro})^{0.5}]$	+	M_6	$\sigma k/[\mu_o v_{w,inj} L(k_{wro})^{0.5}]$	Equation coefficient
Π_7	$\sigma k/[\mu_o v_{w,inj} L(k_{wro})^{0.5}]$	+	M_7	$k_{wro}\,\phi/k$	Equation coefficient
Π_8	$(v_{w,inj}{}^2)(k_{wro}{}^{0.5})\rho_o/\sigma$	+			
Π_9	$(v_{w,inj}{}^2)(k_{wro}{}^{0.5})\rho_w/\sigma$	+			
Π_{10}	$k_{wro}\phi/k$	+			

The complete set of dimensionless parameters generated above as Set No. 17 and selected for the comparison with model parameters is listed as Π_i, i = 1 to 10, on the left side of Table 3, together with each one's variability in the experiments. As show in the table, parameters Π_2, Π_6, Π_7, Π_8, Π_9, and Π_{10} take different values in the analyzed experiments, and four of them are equal to the corresponding model parameters: $\Pi_2 = M_2$, $\Pi_6 = M_5$, $\Pi_7 = M_6$, and $\Pi_{10} = M_7$. Meanwhile, the other two (Π_8 and Π_9) are expected not to influence the experimental results.

It is worth nothing that definite physical meanings can be ascribed to some of the above Π products. They follow from the below relations, (14) and (15):

$$\Pi_{6/7} = \frac{Re_{w/o}}{We_{w/o}}\Pi_1 \tag{14}$$

$$\Pi_{8/9} = \frac{We_{o/w}}{\Pi_1} \tag{15}$$

where $Re_{w/o}$ is the Reynolds number for water/oil, according to Formula (16):

$$Re_{w/o} = \frac{\rho_{w/o}\, v_{w,inj}\, k}{\mu_{w/o}\, L} \tag{16}$$

and $We_{w/o}$ is the Weber number for water/oil, according to Formula (17):

$$We_{w/o} = \frac{\rho_{w/o}\, v_{w,inj}{}^2\, L}{\sigma} \tag{17}$$

As a consequence of Reynolds and Weber number meanings given above, and of the constant value of Π_1, $\Pi_{6/7}$ corresponds to the ratio of interface tension to viscous forces, while $\Pi_{8/9}$ is a measure of the relative importance of the fluid inertia to their interface tension.

It should be noted that values of the parameters Π_6 and Π_7, as well as Π_8 and Π_9, are strongly correlated (co-dependent) in the analyzed experiments. As a consequence, only two of them (Π_6 and Π_8) are taken into account in the dependency analysis below.

6. Experimental Parameters

The basic experimental characteristics are given in Table 4.

Table 4. Basic characteristics of individual experiments.

Parameter Symbol	Parameter Description	Experiment Number				
		1	2	3	4	5
L (cm)	total length of the core assembly	20.18	21.78	20.15	20.11	22.2
t (s)	final time	33.480	35.940	34.200	34.740	61.920
k_{wro} (mD)	water phase permeability at S_{or}	31.500	29.227	26.576	27.523	128.905
k_{orw} (mD)	oil phase permeability at S_{wr}	17.331	16.081	14.622	15.143	70.922
$P_{o,ini}$ (bar)	initial oil pressure	424.62	424.62	424.62	424.62	424.62
$P_{w,ini}$ (bar)	initial water pressure	422.77	422.77	422.77	422.77	422.77
μ_w (g/(cm·s))	water viscosity *	0.0025	0.0025	0.0025	0.0025	0.0025
μ_o (g/(cm·s))	oil viscosity **	0.006	0.006	0.006	0.006	0.006
ρ_o (g/cm^3)	oil density	0.833	0.833	0.833	0.833	0.833
ρ_w (g/cm^3)	water density	1.04	1.04	1.04	1.04	1.04
$v_{w,inj}$ (10^{-4} cm/s)	water injection velocity	1.72	1.74	1.74	1.78	63.3
σ (dyne/cm)	interfacial tension ***	45	45	45	45	45
ϕ (-)	average core porosity	0.251	0.249	0.248	0.243	0.247
k (mD)	average core permeability	49.9	46.3	42.1	43.6	204.2
W_{inj} (fraction of PV)	water injected as fraction of pore volume	1.06	1.06	1.09	1.10	1.08
RF (%)	displacement coefficient	56.1	56.7	56.9	56.9	52.8

* Viscosity from standard correlations under reservoir conditions: T = 119 °C and P = 424 bar [20]. ** Viscosity measured under reservoir conditions: T = 119 °C and P = 424 bar [16]. *** Interfacial tension determined from measurements and standard correlations [21].

Two types of experimental results are used for the quantitative analysis below:

- The relative oil outflow velocity, $v_r = (q_o/A)/v_{w,inj}$, where q_o is the oil outflow rate, and A is the cross section area of the cores;
- The relative total oil outflow, $N = N_p/N_{p,max}$, where N_p is the current total oil outflow, and $N_{p,max}$ is the maximum total oil outflow.

The former quantity is used to analyze the results' dependence upon the temporary parameters (Π_6, Π_7, Π_8, Π_9, and Π_{10}), while the latter is a natural quantity for cumulative parameters (e.g., Π_2).

7. Dependence Analysis

The conventional regression analysis is used to study dependencies of experimental results (v_r and N) upon the dimensionless parameters (Π_2, Π_6, Π_8, and Π_{10}). As regression diagnostic tests, the distributions of both dependent (v_r and N) and independent quantities (Π_2, Π_6, Π_8, and Π_{10}) are determined as their histograms (shown in Figures 2–7) and checked against their normal-like form. The appropriate sets of experimental data points are restricted by rejecting of outliers. In the case of N and Π_2, the residuals of their distributions were shown after subtracting the fitted trends of these quantities.

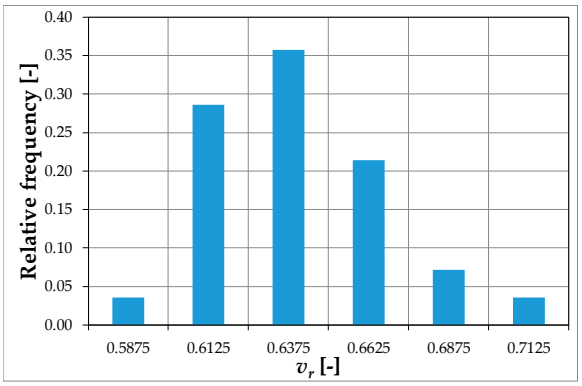

Figure 2. Histogram of v_r.

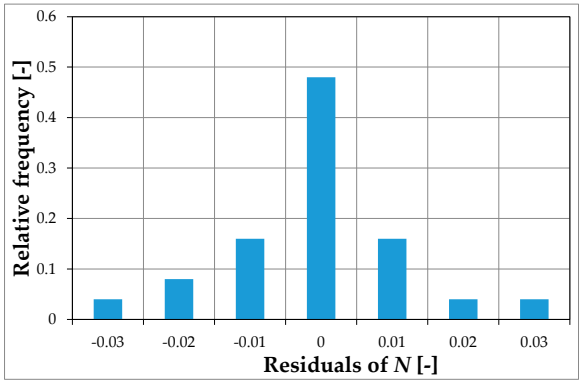

Figure 3. Histogram of N.

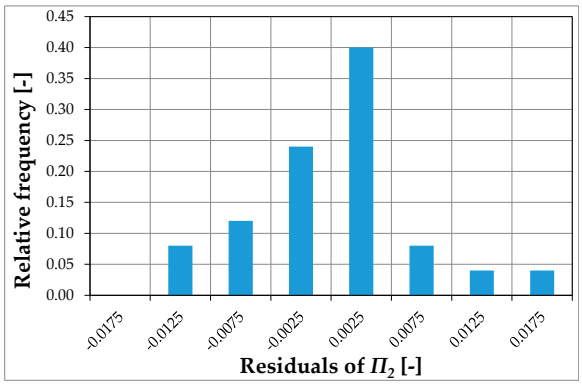

Figure 4. Histogram of Π_2 residuals.

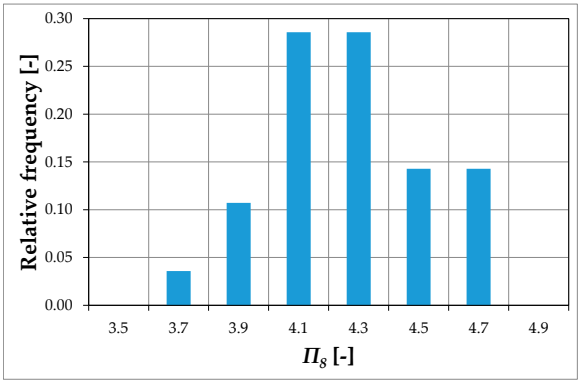

Figure 5. Histogram of Π_8.

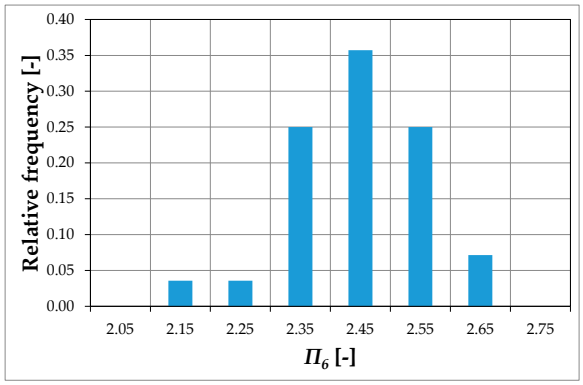

Figure 6. Histogram of Π_6.

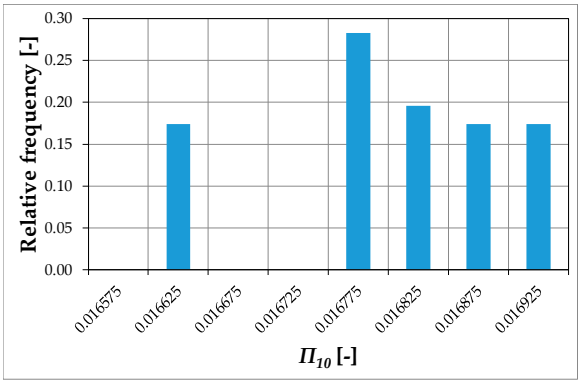

Figure 7. Histogram of Π_{10}.

It is concluded that all the analyzed quantities except Π_{10} satisfy the requirement of their distribution, being appropriate for the conventional linear regression analysis applied to v_r versus Π_6 and Π_8, as well as N versus Π_2.

The analyses of adjusted R square and residual distributions for various models of the regression fitting result in the selection of a bilinear model of v_r vs. Π_8 and Π_6 and a quadratic model of N vs. $1/\Pi_2$ (the reversal of Π_2). Detailed results of the regression analysis are presented in Tables 5 and 6 for v_r and N, respectively. Note that the format and entries of these tables follow the generally accepted convention of the regression results. The quality of regression fittings is shown as v_r vs. Π_8 and Π_6, and N vs. Π_2 in Figure 8, Figure 9, and Figure 10, respectively.

Table 5. Regression analysis summary for v_r vs. Π_8 and Π_6.

Regression Statistics						
Multiply R				0.8829		
R square				0.7796		
Adjusted R square				0.7638		
Standard error				0.0513		
Data points				31		
Analysis of variance						
	Df	*SS*	*MS*	*F*	*Significance F*	
Regression	2	0.2611	0.1305	49.5125	6.39×10^{-10}	
Residual	28	0.0738	0.0026			
Total	30	0.3349				
	Coefficients	SE	*t* Stat	*p*-Values	Lower 97%	Upper 97%
Intersect	0.5516	0.2452	2.2494	0.0325	−0.0091	1.1122
Π_8	−0.0614	0.0282	−2.1800	0.0378	−0.1258	0.0030
Π_6	0.1460	0.0547	2.6698	0.0125	0.0210	0.2709

Table 6. Regression analysis summary for N vs. Π_2.

Regression Statistics						
Multiply R				0.9742		
R square				0.9491		
Adjusted R square				0.9438		
Standard error				0.0091		
Data points				22		
Analysis of variance						
	Df	*SS*	*MS*	*F*	*Significance F*	
Regression	2	0.0295	0.0147	177.2488	5.145×10^{-13}	
Residual	19	0.0016	0.0001			
Total	21	0.0310				
	Coefficients	SE	*t* Stat	*p*-Values	Lower 97%	Upper 97%
Intersect	0.9503	0.0350	27.1592	0.0000	1.0323	0.8682
$1/\Pi_2$	0.0354	0.0141	2.5167	0.0210	0.0684	0.0024
$1/{\Pi_2}^2$	−0.0061	0.0013	−4.5613	0.0002	−0.0030	−0.0093

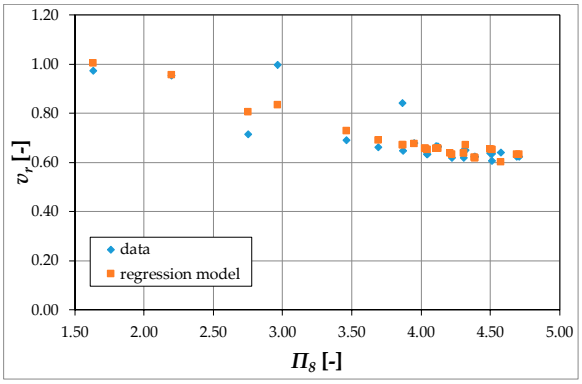

Figure 8. Regression of v_r vs. Π_8.

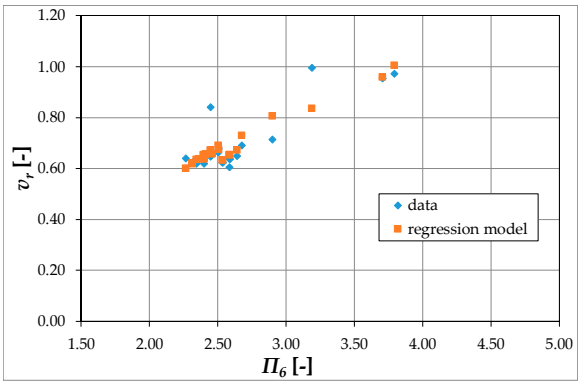

Figure 9. Regression of v_r vs. Π_6.

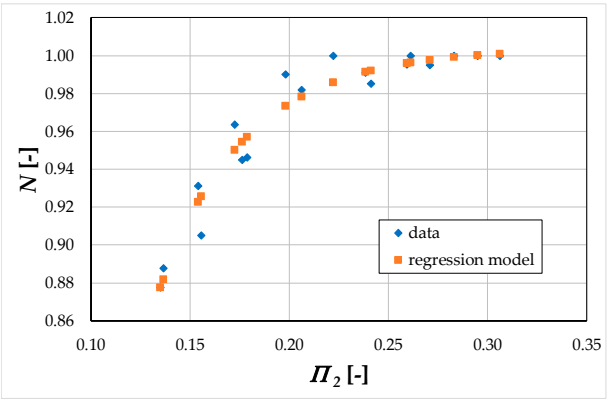

Figure 10. Regression of N vs. Π_2.

The main results of the regression analysis imply that the experimental results for the oil output velocity, v_r, depend in the significantly higher degree on Π_6 (p-value = 0.0125) than on Π_8 (p-value = 0.0378). According to the physical meanings of the products given in Section 5, the experimental results for the oil output velocity, v_r, are determined mostly by the relationship between interfacial tension and viscous forces, while they are weakly dependent upon the ratio of inertial forces to the interfacial tension. The latter dependence results from both the low flow velocity of the reservoir fluids observed in the displacement experiments ($\Pi_8 \sim {v_{w,inj}}^2$) and a large value of Π_1 ($\Pi_8 \sim \frac{1}{\Pi_1}$, $\Pi_1 \approx 1 \times 10^6$).

The analysis of N vs. Π_2 shows the significant dependence of the total oil production upon the quadratic function of $1/\Pi_2$ (with p-value = 0.0210 for linear term and p-value = 0.0002 for quadratic term). Because Π_2 has a direct meaning of the relative range of displacing fluid (injected water), the above quadratic dependence of N vs. Π_2 indicates dispersive effects of the displacement process.

The above results lead to the following conclusions:

- The experimental results are consistent with the model predictions, i.e., explicit dependence upon the following:

  (1) Model coefficients Π_6 (and Π_7);
  (2) Model independent variables (experiment duration) Π_2—linear dependence on Π_2.

- The dependence of experimental results upon other parameters (such as Π_8 and Π_9) that do not enter the model description are much weaker and may be explained by small effects from the inertial forces under the conditions of small fluid velocities; in principle, including inertial effects goes beyond the Darcy law of fluid flow in the porous media.

- Non-linear dependence of the total oil outflow upon the displacement time cannot be taken into account in a simple 1D flow model with no dispersion effects; a typical smoothing-out of the displacement front obtained from such models results from a numerical dispersion defect of the standard numerical solvers of the flow equations; the correct modelling of the physical dispersion effect, responsible for the above mentioned non-linear dependence of the total oil outflow upon the displacement time, can be achieved by applying 3D model of non-uniform transport properties of the porous media and by explicit modelling of the physical dispersion effects.
- The last two points indicate deficiency of the modelling approach analyzed in the paper.

8. Summary and Conclusions

Correctness of using numerical modelling to quantitatively characterize the immiscible displacement phenomenon occurring in the water–oil system was discussed in the paper by studying the results of experimental tests on core sets with scaling and dimensional analysis. To this end, a complete procedure including generation of dimensionless Π products as of the Buckingham Π theorem, identifying the dimensionless parameters of the models, and regression analyses of the experimental results dependence upon the dimensionless Π products were applied.

The following conclusions were drawn from the obtained results:

- Using conventional mathematical flow description and 1D approximation, it is reasonable to model laboratory tests of immiscible displacement in the water-oil system of bore-hole cores.
- The experimental results are consistent with the model predictions, i.e., they significantly depend upon the following:
    - Explicit model coefficients (Π_6 and Π_7) related with the ratio of the Reynolds number to the Weber number that is a measure of the relationship between interfacial tension and viscous forces;
    - Model independent variables (experiment duration—Π_2).
- The dependence of experimental results upon other parameters ((Π_8 and Π_9—corresponding to the ratio of inertial forces to the interfacial tension—the Weber number) that do not explicitly enter the model description is much weaker and results from both the low flow velocity of the reservoir fluids observed in the displacement experiments ($\Pi_{8/9} \sim {v_{w,inj}}^2$) and a typically large value of Π_1 parameter ($\Pi_{8/9} \sim \frac{1}{\Pi_1}$, $\Pi_1 \approx 1 \times 10^6$).
- Non-linear dependence of the total oil outflow upon the displacement time (Π_2) cannot be taken into account in a simple 1D flow model with no dispersion effects.
- The last two observations show the imperfection of the standard modelling approach used to analyze the immiscible displacement of oil by water in porous media.
- The potential way of model improvements consists in including the following:
    - Inertial effects beyond the Darcy law of fluid flow in the porous media;
    - Physical dispersion effects by applying 3D model of non-uniform transport properties of the porous media and by explicit modelling of the dispersion phenomena.

Author Contributions: Conceptualization, J.S., W.S., and A.G.; methodology, A.G. and W.S.; software, A.G.; validation, W.S.; formal analysis, A.G.; investigation, A.G., and P.Ł.; resources, A.G.; data curation, P.Ł. and A.G.; writing—original draft preparation, A.G.; writing—review and editing, W.S.; visualization, A.G. and P.Ł.; supervision, W.S.; project administration, A.G. All authors have read and agreed to the published version of the manuscript.

Funding: The paper was prepared on the basis of a statutory work entitled "Modelling the effects of immiscible displacement using similarity criteria"—INiG-PIB report to the order of the Ministry of Science and Higher Education, archive no. DK-4100-20/19, INiG-PIB internal order no. 30/KZ.

Conflicts of Interest: The authors declare no conflict of interest.

Nomenclature

A	cross-section area of the cores
g	acceleration of gravity
$J(S_w^*)$	J-Leverette function
k	absolute permeability
$k_{w/o}$	water/oil phase permeability
k_{orw}	oil permeability at irreducible water saturation, S_{wr}
k_{wro}	water permeability at residual oil saturation, S_{or}
L	total length of the core assembly length dimension
M	mass dimension
$M_1, M_2, M_3, M_4, M_5, M_6, M_7$	dimensionless model parameters
N	number of observations relative total oil outflow
n	number of physical variables
N_p	current total oil outflow
$N_{p,max}$	maximum total oil outflow
P_c	capillary pressure
$P_{o/w}$	oil/water phase pressure
$P_{o/w,ini}$	initial oil/water pressure
$P_{o/w,out}$	outflow oil/water pressure
$P^*_{o/w}$	dimensionless oil/water phase pressure
q_o	oil outflow rate
$S_{o/w}$	oil/water saturation
$S^*_{o/w}$	reduced oil/water saturation
$S_{o/w,r}$	residual oil/water saturation
t	final time of experiment performance time independent variable
t^*	dimensionless time independent variable
T	temperature
v_r	relative oil outflow velocity
$v_{w,inj}$	water injection velocity
x, y, z	coordinates independent variables
x^*	dimensionless x-coordinate variables
Symbols	
ϕ	porosity
$\Phi_{o/w}$	oil/water potential
$\Delta\rho$	difference of fluid densities
$\mu_{o/w}$	oil/water viscosity
$\Pi_1,\Pi_2,\Pi_3,\Pi_4,\Pi_5,\Pi_6,\Pi_7,\Pi_8,\Pi_9,\Pi_{10}$	dimensionless Π products
$\rho_{o/w}$	oil/water density
σ	oil–water interface tension

References

1. Holstein, E.D. *Volume V—Reservoir Engineering and Petrophysics*; Society of Petroleum Engineers: Richardson, TX, USA, 2007; ISBN 978-1-55563-120-8.
2. Szott, W.; Miłek, K. Application of Reservoir Simulations for Comparative Analysis of EOR for Selected Methods. *Nafta-Gaz* **2015**, *3*, 167–175.
3. Arab, D.; Kantzas, A.; Torsæter, O.; Bryant, S.L. *A Core Scale Investigation of Drainage Displacement*; Society of Petroleum Engineers: Richardson, TX, USA, 2020. [CrossRef]
4. Batycky, J.P.; Mirkin, M.I.; Besserer, G.J.; Jackson, C.H. *Miscible and Immiscible Displacement Studies on Carbonate Reservoir Cores*; Petroleum Society of Canada: Calgary, AB, Canada, 1981. [CrossRef]
5. Hamdy, A.; Samir, M.; Mohamed, K.; El-hoshoudy, A.N. Evaluation of Waterflooding; Experimental and Simulation Overview. *Pet. Petrochem. Eng. J.* **2019**, *3*. ISSN 2578-484. [CrossRef]
6. Lubaś, J.; Szott, W.; Dziadkiewicz, M. Analysis of a Possible Increase of Oil Recovery from Oil Fields in Poland. *Nafta-Gaz* **2012**, *8*, 481–489.

7. Perkins, F.M.; Collins, R.E. *Scaling Laws for Laboratory Flow Models of Oil Reservoirs*; Society of Petroleum Engineers: Richardson, TX, USA, 1960. [CrossRef]
8. Demetre, G.P.; Bentsen, R.G.; Flock, D.L. *A Multi-Dimensional Approach to Scaled Immiscible Fluid Displacement*; Petroleum Society of Canada: Calgary, AB, Canada, 1982. [CrossRef]
9. Buckingham, E. On physically similar systems; illustrations of the use of dimensional equations. *Phys. Rev.* **1914**, *4*, 345–376. [CrossRef]
10. Durst, F. Similarity Theory. In *Fluid Mechanics. An Introduction to the Theory of Fluid Flows*; Springer: Berlin/Heidelberg, Germany, 2008; pp. 193–219, ISBN 978-3-540-71342-5.
11. Cengel, Y.A.; Cimbala, J.M. *Fluid Mechanics: Fundamentals and Applications*; McGraw Hill: Boston, MA, USA, 2010; pp. 291–292.
12. Akers, A.; Gassman, W.; Smith, R. *Hydraulic Power System Analysis*; Taylor & Francis: New York, NY, USA, 2006; Chapter 13; ISBN 0-8247-9956-9.
13. Anderson, J.D., Jr. *Fundamentals of Aerodynamics*, 3rd ed.; McGraw Hill: Boston, MA, USA, 2001; ISBN 0-07-237335-0.
14. Stokes, G. On the Effect of the Internal Friction of Fluids on the Motion of Pendulums. *Trans. Camb. Philos. Soc.* **1851**, *9*, 8–106.
15. Day, P.; Manz, A.; Zhang, Y. *Microdroplet Technology: Principles and Emerging Applications in Biology and Chemistry*; Springer Science & Business Media: Berlin/Heidelberg, Germany, 2012; p. 9, ISBN 978-1-4614-3265-4.
16. Warnecki, M.; Wojnicki, M. *Immiscible Displacement Studies on Borehole Long Cores*, 2010; unpublished work.
17. Szott, W.; Łętkowski, P.; Kwilosz, T.; Pańko, A.; Rychlicki, A. *Optimization of the Conditions for the Production of Reservoir Fluids, Task 7.2: Construction of the Geological Model of the BMB Reservoir*, 2004; unpublished work.
18. Greenkorn, R.A. *Flow Phenomena in Porous Media—Fundamentals and Applications in Petroleum, Water and Food Production*; Marcell Dekker: New York, NY, USA, 1983; ISBN 0-8247-1861-5.
19. Dake, L.P. *Fundamentals of Reservoir Engineering*; Elsevier Science Publishers: Amsterdam, The Netherlands, 1978; ISBN 0-444-41830-X.
20. Amyx, J.W.; Bass, D.M.; Whiting, R.L. *Petroleum Reservoir Engineering. Physical Properties*; Mc Graw-Hill Book Company, Inc.: New York, NY, USA, 1960.
21. Szott, W.; Gołąbek, A.; Miłek, K.; Rychlicki, A. *Report on the Modelling of Laboratory Displacements Tests in Core Samples*; 2019; unpublished work.